IJCRT.ORG ISSN : 2320-2882

INTERNATIONAL JOURNAL OF CREATIVE RESEARCH THOUGHTS (IJCRT)

An International Open Access, Peer-reviewed, Refereed Journal

Cache-Enabled Cognitive Non-Orthogonal Multiple Access with SWIPT over Rayleigh fading channels

[1]Jonnalagadda Sravani (J.Sravani), [2]Md.Asim Iqbal

Department: M.Tech department of Electronics & Communication Engineering , Kakatiya University college of engineering and technology, Warangal, Telengana, India

Assistant professor department of Electronics & Communication Engineering, Kakatiya University college of engineering and technology, Warangal, telengana, India

ABSTRACT

In this research, we suggest using non-orthogonal multiple access (NOMA) for the Internet of Things with cache-enabled coordinated direct and relay (CDRT) transmission (IoT). In order to maximise spectrum use and decrease power consumption, it employs time-switching (TS)-based SWIPT technology in conjunction with overlay cognitive radio (CR). The suggested architecture features a primary network with a primary transmitter and the specified receivers (UE1 and UE2), as well as a secondary network featuring an energy-constrained transmitter, its cache memory, and the receiver it is meant for (IoT-U). The primary transmitter has direct communication with the strong user equipment (UE)1, while the secondary transmitter acts as an Internet of Things (IoT) relay to reach the weak user equipment (UE)2. To relay both the weak user's and its own data, the IoT-transmit node employs a TS-based receiver architecture and a decode-and-forward protocol, in accordance with the NOMA principle. Data from the most frequently accessed files is also prefetched by the cache. Taking into consideration both perfect and imperfect consecutive interference cancellation at the legitimate users over Rayleigh fading channel fading, the proposed system's performance is tested in terms of outage probability, throughput, and energy efficiency. Further, we investigated the potential for primary and secondary networks to work together using a content caching technique to maximise spectrum use. The significance of the most influential criteria is also emphasised, providing a road map for the realistic development of cutting-edge wireless communication networks with minimal influence on either energy consumption or radio frequency bandwidth.

Keywords: Cognitive radio network, coordinated direct and relay transmission, nonorthogonal multiple access, simultaneous wireless information and power transfer, content caching, outage probability.

1. INTRODUCTION

Due to its ability to wirelessly link physical things through applications like BANs, D2Ds, and V2Vs, the Internet of Things (IoT) has received a lot of attention in recent years (V2V). Consequently, the IoT is a significant technology that enables us to create a wide variety of web-based applications. Internet of Things (IoT) is a system that links physical objects to the virtual world. It's a clever method that cuts down on both manual labour and the need for direct access to real tools. With a high density of networked devices, however, spectrum consumption grows exponentially, leading to a scarcity of available frequencies [5]. Key technologies like as cognitive radio (CR) and non-orthogonal multiple access (NOMA) allow enormous device connectivity with greater spectrum efficiency while addressing the problem of spectrum scarcity (SE). Along with NOMA technology, one more promising technology that deals with spectrum usage is Cognitive Radio Network (CRN). It was initially shown in [6] that NOMA is a specific case of CRN, in which the user with the better channel condition is called the strong user and the person with the poorer channel condition is called the weak user. Through the application of CR technology, secondary and primary users can share the same spectrum bands while reducing the occurrence of interference and collision, hence increasing the SE measures [7]. NOMA is a promising technology that enhances SE by a large factor,

and it is one of many alternatives to 5G communications. Due of this, NOMA is a potentially useful protocol for IoT sensor networks [8]. The idea behind NOMA is to employ superposition coding to multiplex signals from different users at the transmitter, and then use successive interference cancellation (SIC) to decode the signals in the power domain at the receiver [9].

The incorporation of NOMA into CR allows for the prospect of higher SE while simultaneously minimising the complexity of the power allocation (PA) design, as described by Cognitive NOMA (CNOMA) [10]. With its high throughput, widespread connection, and low latency, it has the ability to meet the needs of a 5G wireless network. Research efforts centred on CNOMA's implementation using underlay [11], [12] and overlay [13], [15] CR methods have amassed a large body of literature. In [11], the usage of large-scale underlay CR networks with the NOMA approach was explored to boost secondary users' connectivity (SUs). The studies showed that when target data rates and the PA factor were carefully considered, the NOMA users outperformed the OMA users. The outage performance of SU in a CNOMA underlay network is investigated in [12] using the decode-and-forward (DF) relaying protocol. The secondary transmitter (ST) acts as a relay for the primary user (PU) and communicates with its intended secondary receivers (SRs) under the overlay CNOMA paradigm (referenced in [13], [14]). The authors have also looked into the efficiency of an overlay CNOMA system designed specifically for the Internet of Things.

2. EXPLOITING CACHE-FREE/ CACHE-AIDED SWIPT SYSTEM MODEL

2.1. Introduction:

Wireless Caching is an important technique used in present and future wireless networks. Caching at the wireless edge is a unique way of boosting spectral efficiency and reduces energy consumption of wireless systems. The effectiveness of a non-orthogonal multiple access (NOMA) - cache-aided simultaneous wireless information and power transfer (SWIPT) system in relaying data from a source or base station to users at a greater distance. To increase the relay serving time, the relay is assumed to be incorporated with a caching and an energy harvesting (EH) capability. Using a time switching method, we examine how caching impacts the system's throughput and energy efficiency.

2.2. System Model:

2.2.1 Description:

In the proposed system model we incorporate cache memory in relay node along with energy harvesting capability. The advantage of using cache at relay node is that we can reduce the data access delay. This caching scheme can actively pre-fetches the contents from base station or server during off-peak hours and serve the users that can help in the reduction of data access delay. We work to improve the secondary user's transmission rate within the bounds imposed by the primary user's. In fig(2.1), it is presumed that the primary and secondary networks cooperate to exchange cached data. In this setup, we examine a primary network with a single IoT-U and a relay node serving as a secondary transmitter ST, in addition to a primary system with one BS and two PU (primary near user UE1 and primary distant user UE2). In cache free system model we ignore the cache memory block in relay node i.e., in cache free system model relay is equipped with only energy harvesting capability.

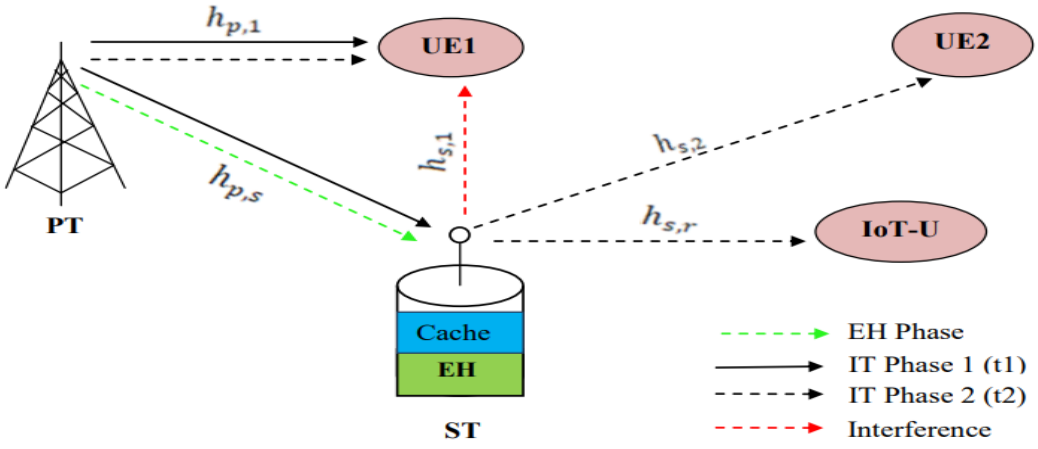

Fig 2.1: Proposed SWIPT based NOMA CDRT system with cache for a single cluster

We assume that the relay, or secondary transmitter node, can detect its surrounding spectrum. When the primary network's transmitter or base station is turned off or otherwise unable to serve primary users, the secondary network can make use of some of the first network's licenced spectrum. Here, it is assumed that all channels exhibit Rayleigh fading. As can be seen in fig. 1, the TSC protocol is employed in both the energy harvesting (EH) and information transfer (IT) processes in this setup (2.2).

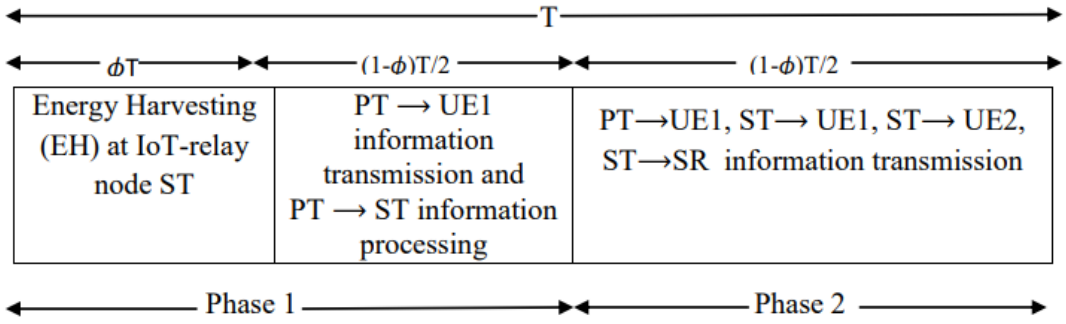

Fig 2.2: Time Switching Protocol with EH and IT Phases

This TS protocol uses a three-part transmission block time T, where (0, 1) represents the TSC parameter. Here, first time phase is divided into two sub-parts based on time splitting factor . In the first time, base station sends information to both UE1 and relay node by exploiting NOMA principle.

2.3 Cache Free SWIPT System Model:

In this model, we ignore the cache memory and follow NOMA- CDRT using time switching protocol.

2.3.1. Energy Harvesting (EH) Phase :

This is the energy collected at ST during the EH phase.

$$E_h = \eta\, \phi\, P_P |h_{ps}|^2 T \quad (1)$$

Where $\eta \in$ P is the transmit power from the source and is the energy conversion efficiency, which depends on the EH circuitry and the rectification procedure. This allows us to derive the formula for node S's transmission power over T /2:

$$P_s = \frac{E_h}{(1-\phi)\, T/2} = \frac{2\, \eta\, \phi\, P_P |h_{ps}|^2}{(1-\phi\,)} \quad (2)$$

2.3.2. Information Transmission (IT) Phase:

In the model of the system that has been proposed, there are two stages of information transmission, each of which needs its own time slot. NOMA transmission method is used in both stages. Phase 1 of IT is represented by the symbol t1, while Phase 2 of IT is represented by the symbol t2.

During t1 phase, base station transmits its composite signal $X_p = \sqrt{\psi_1 P_p} x_1 + \sqrt{\psi_2 P_p} x_2$ to node UE1 using downlink NOMA transmission principle. Here, ψ_1 and x_1 re power allocation factor and data symbol related to UE1 whereas ψ_2 and x_2 are the power allocation factor and data symbol related to UE2 respectively and assuming x_2 as high powered symbol compared to x_1 thus, we can write $\psi_2 > \psi_1$ and $\psi_1 + \psi_2 = 1$. Thus, the received signals at node j, j ∈ (1,s) can be given as

$$y_{(p,1)} = X_p h_{p1} + n_{p1} \quad (3)$$

and the signal received at relay node is given by

$$y_{(p,s)} = \left(\sqrt{(\psi_1 P_p} x_1 + \sqrt{\psi_2 P_p} x_2\right) h_{p1} + n_{ps} \quad (4)$$

Where $n_{p,j}$ is the AWGN variable with variance σ^2 . Considering the NOMA principle, UE1 performs SIC to decode the x_1 symbol. Initially, UE1 decodes x_2 symbol assuming x_1 as noise and then, after performing SIC, x_1 symbol is decoded at UE1. Hence, the SINR received at UE1 to decode x_2 can be expressed as

$$\gamma_{x_2 \to p,1}^{t_1} = \frac{\psi_2 \eta_p |h_{p,1}|^2}{\psi_1 \eta_p |h_{p,1}|^2 + 1} \quad (5)$$

and UE1 to decode x_1 can be given as

$$\gamma_{p,1}^{t_1} = \frac{\psi_1 \eta_p |h_{p,1}|^2}{\lambda \psi_2 \eta_p |h_{p,1}|^2 + 1} \quad (6)$$

$$\gamma_{p,1}^{t_1} = \frac{\psi_1 \eta_p |h_{p,1}|^2}{\lambda \psi_2 \eta_p |h_{p,1}|^2 + 1} \quad (7)$$

where $\eta_p = \frac{P_P}{\sigma^2}$ is the transmit SNR at primary transmitter and $\boldsymbol{\lambda}$ ($0 < \boldsymbol{\lambda} < 1$) is the residual interference parameter when $\boldsymbol{\lambda}$=0 it represents pSIC.

Moreover, IoT-relay will decode x_2 symbol by assuming x_1 as noise since it is a low powered symbol. Thus, the received SINR at IoT- relay node is given by

$$\gamma_{p,s}^{t_1} = \frac{(1-\phi)\psi_2 \eta_p |h_{p,s}|^2}{(1-\phi)\psi_1 \eta_p |h_{p,s}|^2 + 1} \quad (8)$$

In the next IT phase 2 (t2), if ST is able to decode symbol x_2 at t1 then only secondary transmission will take place, otherwise ST will remain silent and no transmission takes place during this phase.

Following successful decoding of x_2 at node ST, it combines x_2 with its own signal x_r to create a composite signal $X_s = \sqrt{\psi_2 P_s} x_2 + \sqrt{\psi_r P_s} x_r$ by using NOMA principle, where ψ_2 and x_2 are power allocation coefficient and data symbol related to UE2 whereas ψ_r and x_r are the power allocation coefficient and data symbol related to IoT-U respectively and assuming x_2 as high powered symbol compared to x_r thus, we can write $\psi_2 > \psi_r$ and $\psi_2 + \psi_r = 1$. As a result, we may write down the signal strength as

$$y_{sj} = X_s h_{sj} + n_{sj} \quad (9)$$

where $n_{s,j}$ is the AWGN variable and $j \in (2,r)$. Here, x_2 can be directly decoded at UE2 because of high power allocation, whereas SIC is employed to decode x_r at IoT-U. It first decodes x_2 considering x_r as noise and then decodes x_r by discarding x_2 using SIC. Therefore, the SINR received at UE2 to decode x_2 can be given as

$$\gamma_{s,2}^{t_1} = \frac{\psi_2 \delta \eta_p |h_{p,s}|^2 |h_{s,2}|^2}{\psi_r \delta \eta_p |h_{p,s}|^2 |h_{s,2}|^2 + 1} \quad (10)$$

where $\delta = \eta \phi$

For the secondary network, the received SINR at SR to decode $\boldsymbol{x_2}$ before decoding $\boldsymbol{x_r}$ is given by

$$\gamma_{x_2 \to s.r}^{t_2} = \frac{\psi_2 \delta \eta_p |h_{p,s}|^2 |h_{s,r}|^2}{\psi_r \delta \eta_p |h_{p,s}|^2 |h_{s,r}|^2 + 1} \quad (11)$$

The received SINR at IoT-U to decode x_r after SIC can be given as

$$\gamma_{s,r}^{t_2} = \frac{\psi_r \delta \eta_p |h_{p,s}|^2 |h_{s,r}|^2}{\lambda \psi_2 \delta \eta_p |h_{p,s}|^2 |h_{s,r}|^2 + 1} \quad (12)$$

In order to maximize spectral utilization and the wireless channel, source node PT transmits the new signal $\hat{x}_1$ to UE1 with transmit power $\sqrt{\psi_1^{t_2} P_p}$, $\psi_1^{t_2} \in (0, 1)$. However, during t2, UE1 faces the interference from IoT-relay node ST, which can be estimated and eliminated by using the side information of x_2 that is obtained through SIC process during t1.

Therefore, the signal received at UE1 during t2 is given by

$$y_{(p,s),1}^{t_2} = \sqrt{\psi_1^{t_2} P_p} h_{p,1} \hat{x}_1 + h_{s,1} X_s + n_{p1} \quad (13)$$

and corresponding SINR is given, respectively, by

$$\gamma_{p,1}^{t_2} = \frac{\psi_1^{t2} \eta_p |h_{p,1}|^2}{\psi_r \delta \eta_p |h_{p,s}|^2 |h_{s,1}|^2 + 1} \quad (14)$$

3. PERFORMANCE ANALYSIS

Here, we derive analytical expressions over a Rayleigh fading channel to compare the availability of primary and secondary networks. Here, we take the goal rates of R_1, R_2, and R_r for UE1, UE2, and IoT-U, respectively.

3.1 Outage Probability of Primary Network:

3.1.1 Outage Probability of UE1:

During t1 phase, the outage event of primary user1 occurs when UE1 unable to decode both symbols x_1 *and* x_2, and this is given as

$$P_{out,(1,p)}^{t_1} = 1 - P_r\left(\gamma_{x_2 \to p,1}^{t_1} > R_2^{th} \, ; \, \gamma_{p,1}^{t_1} > R_1^{th}\right) \quad (15)$$

where $R_1^{th} = 2^{2R_1} - 1$, $R_2^{th} = 2^{2R_2} - 1$, and by invoking respective SINR model equations into above and performing some mathematical computations on those will result in following outage expression which is given by

$$P_{out,(1,p)}^{t_1} = 1 - P_r\left[|h_{p,1}|^2 > \Delta\right] = Exp\left(-\frac{\Delta}{\Omega_{p1}}\right) \quad (16)$$

where $\Delta = max(u_1, u_2)$ and $u_1 = \frac{R_2^{th}}{(\varphi_2 - \varphi_1 R_2^{th})\eta_p}$, $u_2 = \frac{R_2^{th}}{(\varphi_1 - \lambda \varphi_2 R_2^{th})\eta_p}$

3.1.2. Outage Probability of UE2:

The outage event of the UE2 occurs either UE2 cannot decode its symbol x_2 or the relay node is unsuccessful in decoding. For a predefined target rate R_2 the outage probability of UE2 is given as below.

$$P_{out,UE2}^{t_2} = \underbrace{P_r\left(\gamma_{p,s}^{t_1} > R_2^{th} \, ; \, \gamma_{s,2}^{t_2} > R_2^{th}\right)}_{P_1} + \underbrace{P_r\left(\gamma_{p,s}^{t_1} < R_2^{th}\right)}_{P_2} \quad (17)$$

By invoking respective SINR model equations into above and performing some mathematical computations on those will result in following outage expression. The analytical expression for $P_{out,UE2}^{t_2}$ over Rayleigh fading channel conditioned on $R_2^{th} < \frac{\varphi_2}{\varphi_1}$ can be given as $P_{out,UE2}^{t_2} = P_1 + P_2$. Final expression for $P_{out,UE2}^{t_2}$ is given as

$$P_{out,UE2}^{t_2} = \frac{u_4}{\rho_p \Omega_{ps} \Omega_{s2}} ExpIntegralEi[1, \frac{u_3}{\rho_p \Omega_{ps}}] \text{ (18)}$$

where $u_3 = \frac{R_2^{th}}{(\varphi_2 - \varphi_1 R_2^{th})\beta\eta_p}$ and $u_4 = \frac{R_2^{th}}{(\varphi_2 - \varphi_r R_2^{th})\beta\eta_p}$

3.2 Outage Probability of Secondary network:

Only when the secondary transmitter can decode the x_2 symbol will it send data across the secondary network. Both failure to detect symbol x_2 at the ST node and failure to detect symbol x_r at the IoT-relay node constitute an outage event for the IoT-U.

The chance of secondary network failure, for a particular target rate threshold R r, is

$$P_{out,sr}^{t_2} = \underbrace{P_r\left(\gamma_{p,s}^{t_1} > R_2^{th} ; \bar{P}_{sr}\right)}_{P_{out1}} + \underbrace{P_r\left(\gamma_{p,s}^{t_1} < R_2^{th}\right)}_{P_{out2}} \text{ (19)}$$

where $R_r^{th} = 2^{\frac{2\eta R_r}{1-\alpha}}$, $\bar{P}_{sr}$ denotes the OP of IoT-U fails to detect any symbol can be given as

$$\bar{P}_{sr} = 1 - P_r\left(\gamma_{x_2 \to s.r}^{t_2} > R_2^{th} ; \gamma_{s,r}^{t_2} > R_r^{th}\right) \text{ (20)}$$

The analytical expression for $P_{out,sr}^{t_2}$ over Rayleigh fading channel conditioned on $R_2^{th} < \frac{\varphi_2}{\varphi_r}$ can be given as

$$P_{out,sr}^{t_2} = \frac{u_c}{\rho_p \Omega_{ps} \Omega_{s2}} ExpIntegralEi[1, \frac{u_3}{\rho_p \Omega_{ps}}] \text{ (21)}$$

where $u_c = \max(u_5, u_6)$, $u_5 = \frac{R_2^{th}}{(\varphi_2 - \varphi_r R_2^{th})\beta\eta_p}$ and $u_6 = \frac{R_r^{th}}{(\varphi_r - \lambda\varphi_2 R_r^{th})\beta\eta_p}$

3.2.1. Cache Aided SWIPT System Model:

In this model, we include the cache memory and follow NOMA- CDRT using time switching protocol. Here, in cache aided system model we include cache memory at the relay node and based on the system model we assume that cache is assumed to have limited cache capacity. On the basis of this system model and considering transmission block time T into account we formulate a transmission model which helps in evaluating transmission rate.

3.2.2. Transmission Model:

In the data transmission model, we assume a bandwidth of 1MHZ and a primary user's bandwidth allocation of T1 to transfer a requested file. A time slot T/2 is segmented into three sections according to the principal and secondary content cached:

t_p: It is the time taken by the cache to fetch the un-cached primary content for the PU

t_s: It is the time taken by the cache to fetch the un-cached secondary content for the SU

$T_1 - t_p - t_s$: At this point in time, the secondary relay node is sending both the primary and secondary material.

Time required by relay to fetch un-cached primary content for primary user	Time taken by cache in relay node to fetch the un-cached secondary content for secondary user	Time taken by cache in relay node to fetch the un-cached secondary content for secondary user

$\longleftarrow t_p \longrightarrow \longleftarrow t_s \longrightarrow \longleftarrow T_1 - t_p - t_s \longrightarrow$

Fig. 3.1: Time taken by cache memory to fetch un-cached content for PU and SU

Here, we assume the existence of two separate networks, or "main" and "secondary," that are each interested in a different set of data files. Let, $x_p$and x_s be the file-request signals delivered by the primary and secondary transmitters P and ST, respectively; additionally, the relay node commits a sizable percentage of its available power to serving the primary and its own users. The received signal at primary users (UE1,UE2) and secondary user (IoT-U) are given by

$$y_{(s,j)} = \sqrt{\mu\, h_{sj} P_s} x_p + n_{sj} \quad (22)$$

where j={1,2}, Likewise, the signal strength at IoT-U is defined as

$$y_{(s,r)} = \sqrt{(1-\mu) h_{sr} P_s} x_s + n_{sr} \quad (23)$$

where μ and (1-μ) main and secondary users' power allocation coefficients, respectively.

Signal to noise ratio received at primary and secondary users are given by

$$(SNR)_{PU} = \gamma_{pu} = \frac{\mu\, \eta_s\, |h_{sj}|^2}{(1-\mu)\, \eta_s\, |h_{sj}|^2 + 1} \quad (24)$$

$$(SNR)_{SU} = \gamma_{su} = \frac{(1-\mu)\, \eta_s\, |h_{sj}|^2}{(\mu)\, \eta_s\, |h_{sj}|^2 + 1} \quad (25)$$

We hypothesise that during periods of low network activity, the relay's cache will be able to get frequently requested data from both the primary and secondary networks. We classify the transmission model into 4 varieties based on the content cached by primary and secondary users.

Type-1: When the relay has cached copies of both the primary and secondary files requested by the PU and SU, it can serve both clients at once for the duration of the t2 phase (T/2). So, we can write down the PU and SU data transfer rates as

$$R_1^{pu} = R_p . P_r\left(T_1 log_2(1 + (SNR)_{PU} \geq R_{eq}^{th}\right) \quad (26)$$

$$R_1^{su} = R_s . P_r\left(T_1 log_2(1 + (SNR)_{SU} \geq R_{eq}^{th}\right) \quad (27)$$

output expressions for R_1^{pu} and R_1^{su} can be given as

$$R_1^{pu} = R_p \left(1 - 2\left(\frac{\phi_1 \Omega_{ps}}{\Omega_{s1}}\right)^{\frac{1}{2}} K_1\left(2\sqrt{\frac{\phi_1}{\Omega_{s1}\, \Omega_{ps}}}\right)\right) \quad (28)$$

$$R_1^{s} = R_s \left(1 - 2\left(\frac{\phi_1 \Omega_{ps}}{\Omega_{sr}}\right)^{\frac{1}{2}} K_1\left(2\sqrt{\frac{\phi_1}{\Omega_{sr}\, \Omega_{ps}}}\right)\right) \quad (29)$$

Similiarly, transmission rates for type 2, 3 and 4 can be obtained by replacing T_1 with $T_1 - t_s$, $T_1 - t_p$ and $T_1 - t_p - t_s$ respectively.

3.2.3. Transmission Rate:

To maximize the usage of secondary transmitter, we calculate the effective transmission rates of primary and secondary user from ST.

$$R^{su}(C_0, \beta) = p_p . p_s . R_1^{su} + p_p . R_2^{su} + p_s . R_3^{su} + R_4^{su} \quad (30)$$

subject to

$$R^{pu}(C_0,\beta) = p_p.p_s.R_1^{pu} + p_p.R_2^{pu} + p_s.R_3^{pu} + R_4^{pu} \quad (31)$$

$$0 \le t_s \le T_1;\ 0 \le t_p \le T_1;\ 0 \le t_p + t_s \le T_1;\ 0 \le C_0 \le C;\ 0 \le \mu \le 1$$

above equations can be re-written as

$$R^{su}(q,\beta) = \frac{(lc)^{1-\gamma_p}-1}{M^{1-\gamma_p}-1}.\frac{((1-l)c)^{1-\gamma_s}-1}{M^{1-\gamma_s}-1}.R_1^{su} + \frac{(lc)^{1-\gamma_p}-1}{M^{1-\gamma_p}-1}.R_2^{su} \quad (32) + \frac{((1-l)c)^{1-\gamma_s}-1}{M^{1-\gamma_s}-1}.R_3^{su} + R_4^{su}$$

$$R^{pu}(q,\beta) = \frac{(lc)^{1-\gamma_p}-1}{M^{1-\gamma_p}-1}.\frac{((1-l)c)^{1-\gamma_s}-1}{M^{1-\gamma_s}-1}.R_1^{pu} + \frac{(lc)^{1-\gamma_p}-1}{M^{1-\gamma_p}-1}.R_2^{pu} \quad (33) + \frac{((1-l)c)^{1-\gamma_s}-1}{M^{1-\gamma_s}-1}.R_3^{pu} + R_4^{pu}$$

Where γ_p, γ_s are the content file popularities of primary and secondary files respectively.

3.2.4. Caching model:

Here, we assume that the library of files requested by primary and secondary network users as $F_{PU} \cong \{1,2,3,\dots,M\}$ and $F_{SU} \cong \{1,2,3,\dots,N\}$.

We assume, without limiting ourselves to any specific case, that primary and secondary content popularity follows the well-known Zipf law, as described by

$$f_i^{PU} = \frac{i^{-\gamma_p}}{\sum_{n=1}^{M} n^{-\gamma_p}};\ (i \in F_{PU}) \quad (34)$$

$$f_j^{SU} = \frac{j^{-\gamma_s}}{\sum_{n=1}^{N} n^{-\gamma_s}};\ (j \in F_{SU}) \quad (35)$$

In this model, we assume that the file popularity contents of primary and secondary follow descending order and is shown as $f_1^{PU} \ge f_2^{PU} \ge f_3^{PU} \ge \cdots \ge f_M^{PU}$ and $f_1^{SU} \ge f_2^{SU} \ge f_3^{SU} \ge \cdots \ge f_N^{SU}$ with $\sum_{i=1}^{M} f_i^{PU} = 1$ and $\sum_{j=1}^{N} f_j^{SU} = 1$. As we assume that, cache can access some of the contents during off-peak hours due to this, relay can gain more transmission time and secondary transmitter can able to serve both primary and secondary users simultaneously and can lead to successful transmission of the information in the entire network.

Here, we consider that C as the total cache capacity of relay and C_0 is the amount of capacity used to serve the primary content and remaining portion $C - C_0$ is used to serve its own users.

3.3 Performance Analysis:

Analytical expressions are derived over a Rayleigh fading channel with a caching strategy in order to compare the availability of primary and secondary networks. We define R eqth as the rate threshold for UE1, UE2, and IoT-U in this context.

3.3.1. Outage Probability:

Using Cache scheme, outage event of primary user and secondary user occurs in above mentioned four types.

$$(P_{out})_{PU} = p_p.p_s.(P_{out1})_{PU} + p_p.(P_{out2})_{PU} + p_s.(P_{out3})_{PU} + (P_{out4})_{PU} \quad (36)$$

$$(P_{out})_{SU} = p_p.p_s.(P_{out1})_{SU} + p_p.(P_{out2})_{SU} + p_s.(P_{out3})_{SU} + (P_{out4})_{SU} \quad (37)$$

Type-1:

When cache already have the requested file contents of PU and SU, then outage event of PU and SU is given by

$$(P_{out1})_{PU} = 1 - P_r\left(T_1 log_2(1 + (SNR)_{PU} \geq R_{eq}^{th}\right) \quad (37)$$

$$(P_{out1})_{SU} = 1 - P_r\left(T_1 log_2(1 + (SNR)_{SU} \geq R_{eq}^{th}\right) \quad (38)$$

Output expressions for $(P_{out1})_{PU}$ and $(P_{out1})_{SU}$ can be given as

$$(P_{out1})_{PU} = 1 - \left(1 - 2\left(\frac{\phi_1 \Omega_{ps}}{\Omega_{s1}}\right)^{\frac{1}{2}} K_1\left(2\sqrt{\frac{\phi_1}{\Omega_{s1}\,\Omega_{ps}}}\right)\right) \quad (39)$$

$$(P_{out1})_{SU} = 1 - \left(1 - 2\left(\frac{\phi_1 \Omega_{ps}}{\Omega_{s1}}\right)^{\frac{1}{2}} K_1\left(2\sqrt{\frac{\phi_1}{\Omega_{s1}\,\Omega_{ps}}}\right)\right) \quad (40)$$

Similiarly, outage probability expressions for type 2,3 and 4 can be obtained by replacing T_1 with $T_1 - t_s$, $T_1 - t_p$ and $T_1 - t_p - t_s$ respectively.

3.3.2. System Throughput:

System throughput is one of the most useful metrics for gauging spectrum use. In wireless networks based on cooperative communication, it is the average spectral efficiency that is taken into account. Success for the proposed cache free/cache aided SWIPT based NOMA-CDRT system can be described as the sum of the individual target rates for primary and secondary communications over Rayleigh fading channels. System throughput can be expressed as a function of the probability of outages using the following formula

$$S_T = \frac{1}{2}\left[(1 - (P_{out})_{PU})R_{pu} + (1 - (P_{out})_{SU})R_{su}\right] (41)$$

where R_{pu} and R_{su} are the predefined data rates for PU and SU respectively.

3.3.4 Energy Efficiency:

The throughput expression in can be used to calculate the EE for the proposed system (2.59). We evaluate EE by calculating the data delivery rate as a percentage of the total energy used [2.60]. System throughput quantifies the amount of data transferred, and the energy efficiency of the cache-free/cache-aided SWIPT-based CDRT-NOMA system model under consideration can be expressed as

$$E_E = \frac{2\,S_T}{\eta_p} \quad (42)$$

where S_T is the achievable throughput.

4. NUMERICAL AND SIMULATION RESULTS

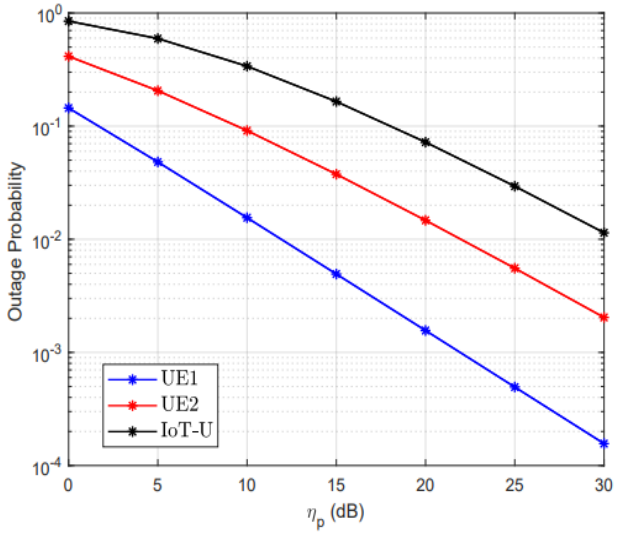

Fig 4.1:OP of SWIPT based NOMA CDRT system over Rayleigh fading channel

In fig(4.1), we have plotted the outage probability of SWIPT based NOMA CDRT system over Rayleigh fading channel by using time switching protocol without using caching scheme. Here, as SNR increases, OP decreases indicates as signal power increases there will be a better performance from the system.

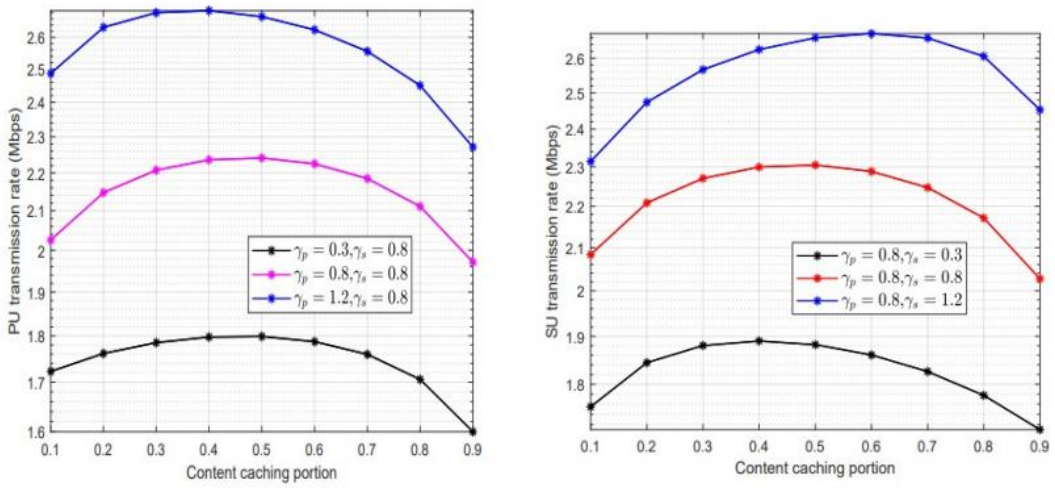

Fig 4.2: Content caching portion versus PU, SU Transmission rate

The pace at which PU and SU transmit their own material is shown in Fig.(4.2) as a function of the caching fraction for three different values of _p and _s. Because the PU prioritises spreading its most popular files as their popularity grows, the primary user sees a significant increase in their transfer speeds as _p rises. In the similar way, for the secondary user IoT-U as γ_s increases, we can achieve more increase in transmission rate.

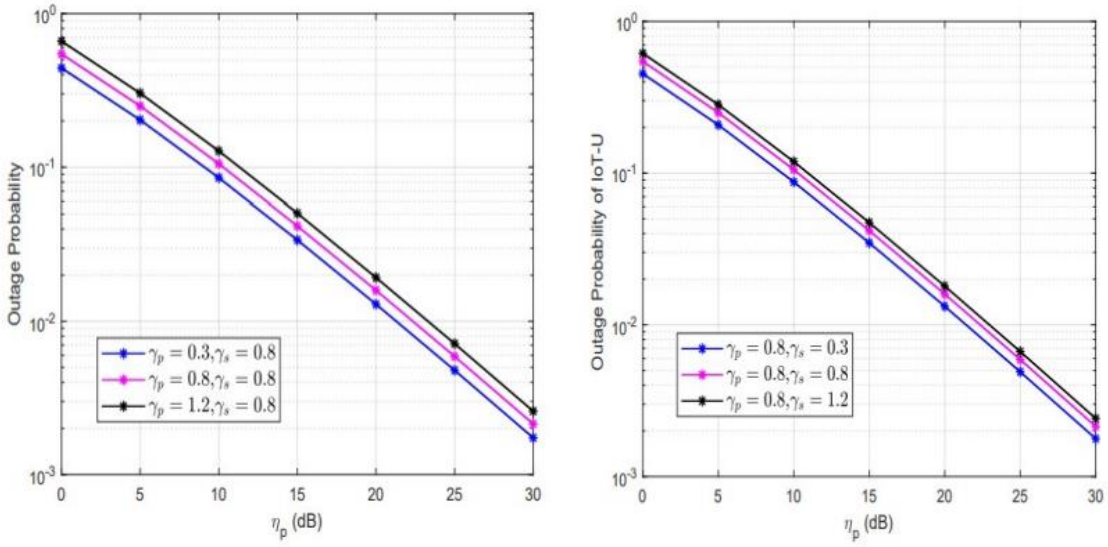

Fig 4.3: Outage Probability of PU and SU versus Transmit SNR

In Fig.(4.3), we analysed the system performance in terms of outage probability, as the η_p(dB) increases the outage probability decreases for both primary and IoT-U and also we can observe that as the file popularity is decreasing there will be a better performance in outage probability.

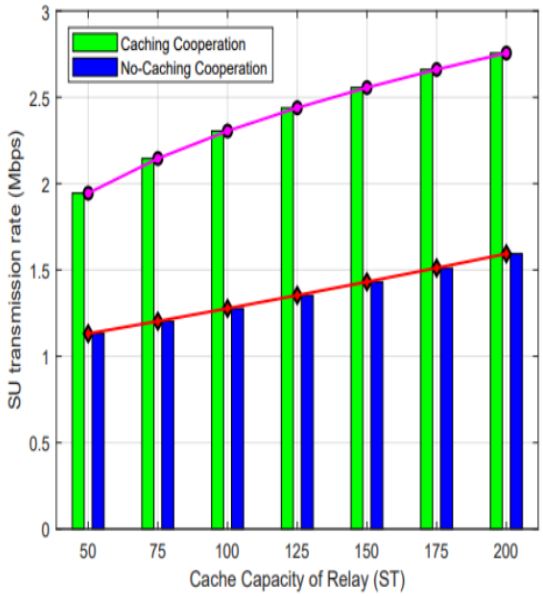

Fig 4.4: Effective achievable transmission rates for different cache capacity

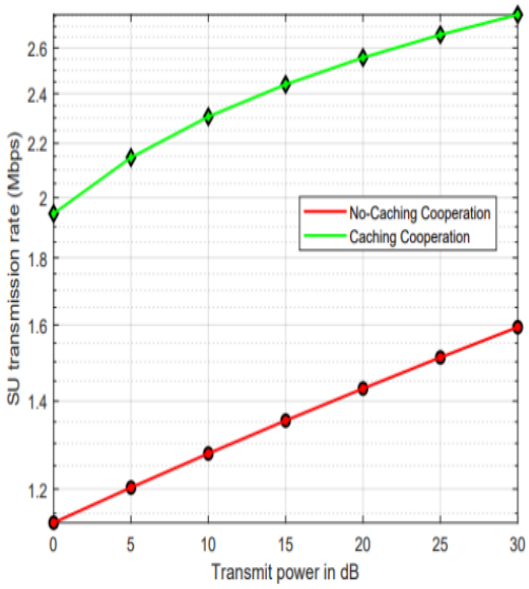

Fig 4.5: IoT-U transmission rate versus transmit power with and without caching scheme

Fig(4.4), shows the impact of different cache capacities on achievable transmission rate of IoT-U. We can expect more SU transmission rate as the capacity C increases, because as we increase C then we can expect more requested content for PU and SU can be transmitted simultaneously, thus we can reduce transmission delay. Cache aided system model provides higher transmission rate compared to cache free system model as shown in fig(4.3).

In fig(4.5), effective transmission rate of secondary user increases as transmit power increases, compared to non-caching scheme, cache scheme will provide more transmission rate. When the transmitted power is increased the primary network reduces the dependency on content caching cooperation so that additional power can be used for SU transmission.

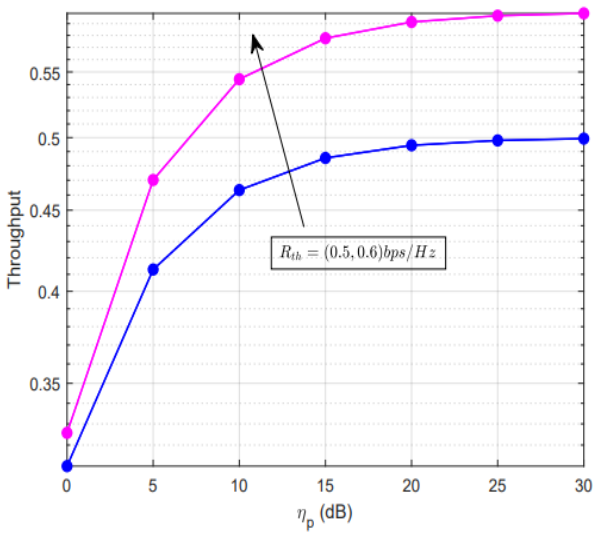

Fig 4.6: Throughput vs η_p in (dB)

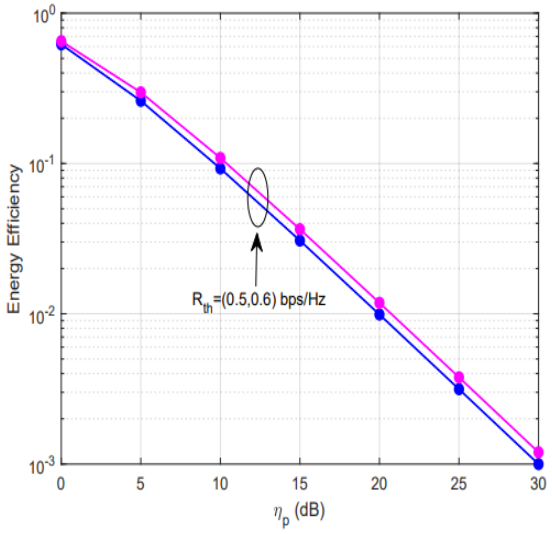

Fig 4.7: Energy efficiency vs η_p in (dB)

In fig(4.6), depicts that as the data rate increasing we could able to observe the improvement in system throughput. Here, we set the data rates $R_1 = R_2 = R_r = 0.5, 0.6\ bps/Hz$. As can be seen in the image, the system throughput improves from a low to medium signal-to-noise ratio (SNR), but then reaches a saturation point at a certain data rate. At a high signal-to-noise ratio, the maximum data rate is achieved. It occurs because outage performance at higher target rates is worse than at lower target rates.

For a given target rate, the maximum EE is achieved at a distinct signal-to-noise ratio, as shown in fig(4.7). When the target rate is altered, so is this. As a result of the fact that, at high SNR, energy consumption is greater than the obtained system throughput, regions with a high SNR have the lowest energy efficiency.

CONCLUSION

In this work, cache enabled SWIPT based NOMA-CDRT using TSC protocol over Rayleigh fading channel fading channel is studied. It analyses and evaluates the proposed system's performance in terms of the likelihood of outages. Monte Carlo simulations are used to verify the accuracy of the results and learn more about the proposed network's outage probability, throughput, and energy efficiency. The effect of tweaking a few settings is also investigated on SWIPT-NOMA CDRT's overall performance. The numerical findings highlighted the significance of using SWIPT-enabled IoT relay which allows independent energy efficient communication and data transmission. We also implemented caching cooperation scheme in SWIPT model with time switching protocol that reduces the data access delay time and improved the transmission rate performance. We also calculated the outage probability, system throughput and energy efficiency using cache model under Rayleigh fading channel that provided a proper comparison between caching and non-caching cooperation schemes.

FUTURE SCOPE

In the proposed system model, the investigation for multi-antenna node, full-duplex, nonlinear EH model, and the ESC arise as a potential future work. Another perk of the caching concept is that it lends itself well to popularity prediction of files via machine learning and big data techniques. However, the findings from this study will serve as a standard and serve as a set of rules for the development of 5G wireless communication in the future.

REFERENCES

[1] A. Al-Fuqaha, M. Guizani, M. Mohammadi, M. Aledhari and M. Ayyash, "Internet of Things: A Survey on Enabling Technologies, Protocols, and Applications," in IEEE Communications Surveys & Tutorials, vol. 17, no. 4, pp. 2347-2376, Fourthquarter 2015, doi: 10.1109/COMST.2015.2444095.

[2] A. K. Shukla, P. K. Upadhyay, A. Srivastava and J. M. Moualeu, "Enabling Co-Existence of Cognitive Sensor Nodes With Energy Harvesting in Body Area Networks," in IEEE Sensors Journal, vol. 21, no. 9, pp. 11213-11223, 1 May1, 2021, doi: 10.1109/JSEN.2021.3062368.

[3] Z. Ding, P. Fan, and H. V. Poor, “Impact of user pairing on 5g nonorthogonal multipleaccess downlink transmissions,” IEEE Transactions on Vehicular Technology, vol. 65, no. 8, pp. 6010–6023, 2016.

[4] Z. Kuang, G. Liu, G. Li and X. Deng, "Energy Efficient Resource Allocation Algorithm in Energy Harvesting-Based D2D Heterogeneous Networks," in IEEE Internet of Things Journal, vol. 6, no. 1, pp. 557-567, Feb. 2019, doi: 10.1109/JIOT.2018.2842738.

[5] S. Kumar, U. Dohare, K. Kumar, D. Prasad Dora, K. Naseer Qureshi and R. Kharel, "Cybersecurity Measures for Geocasting in Vehicular Cyber Physical System Environments," in IEEE Internet of Things Journal, vol. 6, no. 4, pp. 5916-5926, Aug. 2019, doi: 10.1109/JIOT.2018.2872474.

[6] Z. Ding, P. Fan, and H. V. Poor, “Impact of user pairing on 5g non-orthogonal multipleaccess downlink transmissions,” IEEE Transactions on Vehicular Technology, vol. 65, no. 8, pp. 6010–6023, 2016.

[7] M. R. Palattella et al., "Internet of Things in the 5G Era: Enablers, Architecture, and Business Models," in IEEE Journal on Selected Areas in Communications, vol. 34, no. 3, pp. 510-527, March 2016, doi: 10.1109/JSAC.2016.2525418.

[8] S. Haykin, "Cognitive radio: brain-empowered wireless communications," in IEEE Journal on Selected Areas in Communications, vol. 23, no. 2, pp. 201-220, Feb. 2005, doi: 10.1109/JSAC.2004.839380.

[9] L. Chen, B. Hu, G. Xu and S. Chen, "Energy-Efficient Power Allocation and Splitting for mmWave Beamspace MIMO-NOMA With SWIPT," in IEEE Sensors Journal, vol. 21, no. 14, pp. 16381-16394, 15 July15, 2021, doi: 10.1109/JSEN.2021.3076517.

[10] Y. Saito, A. Benjebbour, Y. Kishiyama, and T. Nakamura, “System-level performance evaluation of downlink non-orthogonal multiple access (NOMA),” in IEEE 24th Annual International Symposium on Personal, Indoor, and Mobile Radio Communications (PIMRC), 2013, pp. 611- 615, London, UK.

[11] Y. Liu, Z. Ding, M. Elkashlan, and J. Yuan, “Nonorthogonal multiple access in largescale underlay cognitive radio networks,” IEEE Trans. Veh. Technol., vol. 65, no. 12, pp. 10152-10157, Dec. 2016.

[12] S. Arzykulov, G. Nauryzbayev, T. A. Tsiftsis, B. Maham, and M. Abdallah, “On the outage of underlay CR-NOMA networks with detectand-forward relaying,” IEEE Trans. Cogn. Commun. Netw., vol. 5, no. 3, pp. 795-804, Sep. 2019.

[13] L. Lv, Q. Ni, Z. Ding, and J. Chen, “Application of non-orthogonal multiple access in cooperative spectrum-sharing networks over Rayleigh fading channel fading channels,” IEEE Trans. Veh. Technol., vol. 66, no. 6 , pp. 5510- 5515, Jun. 2017.

[14] L. Luo, Q. Li, and J Cheng, “Performance analysis of overlay cognitive NOMA systems with imperfect successive interference cancellation,” IEEE Tran. Commun., vol. 68, no. 8, pp. 4709-4722, Aug. 2020.

[15] C. K. Singh and P. K. Upadhyay, “Overlay cognitive IoT-based fullduplex relaying NOMA systems with hardware imperfections,” IEEE Internet Things J., doi: 10.1109/JIOT.2021.3111124.